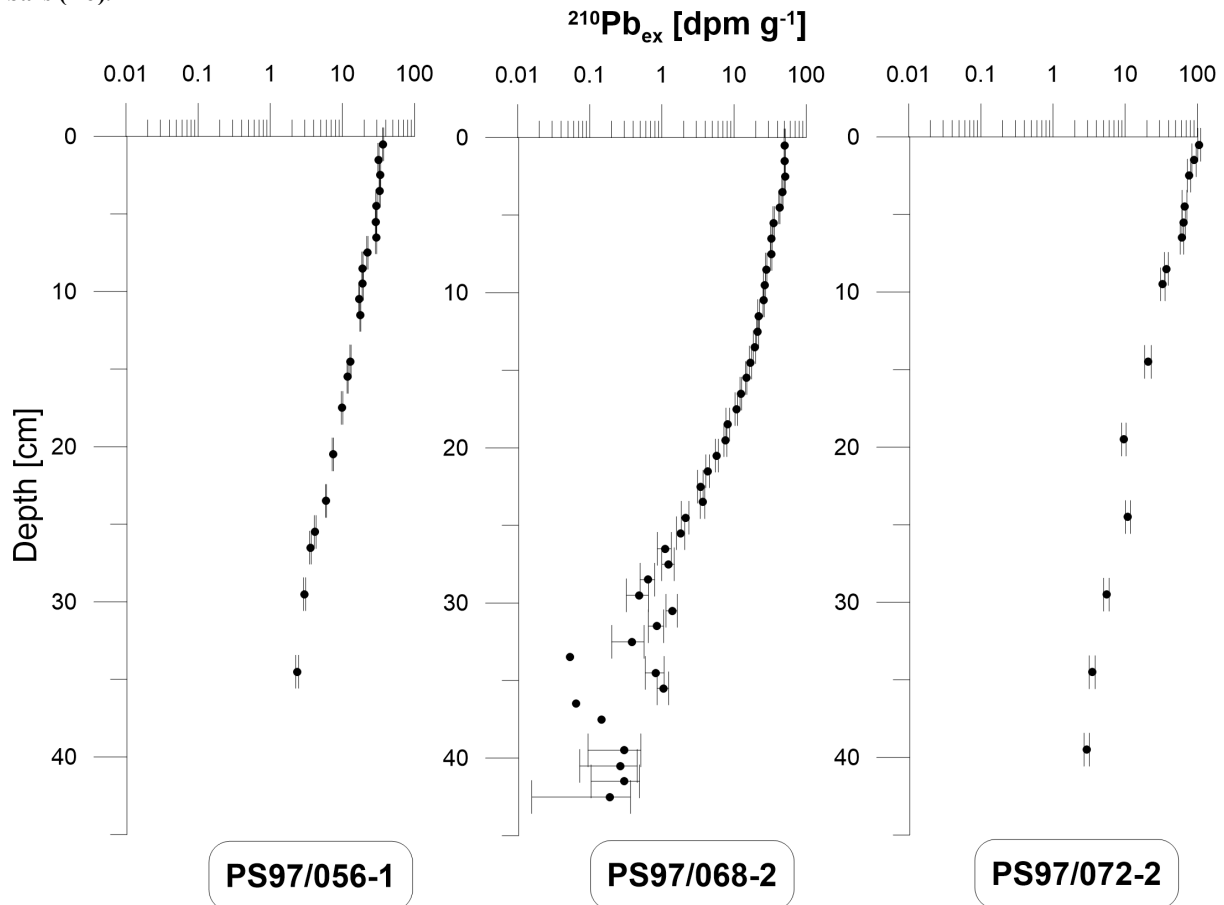


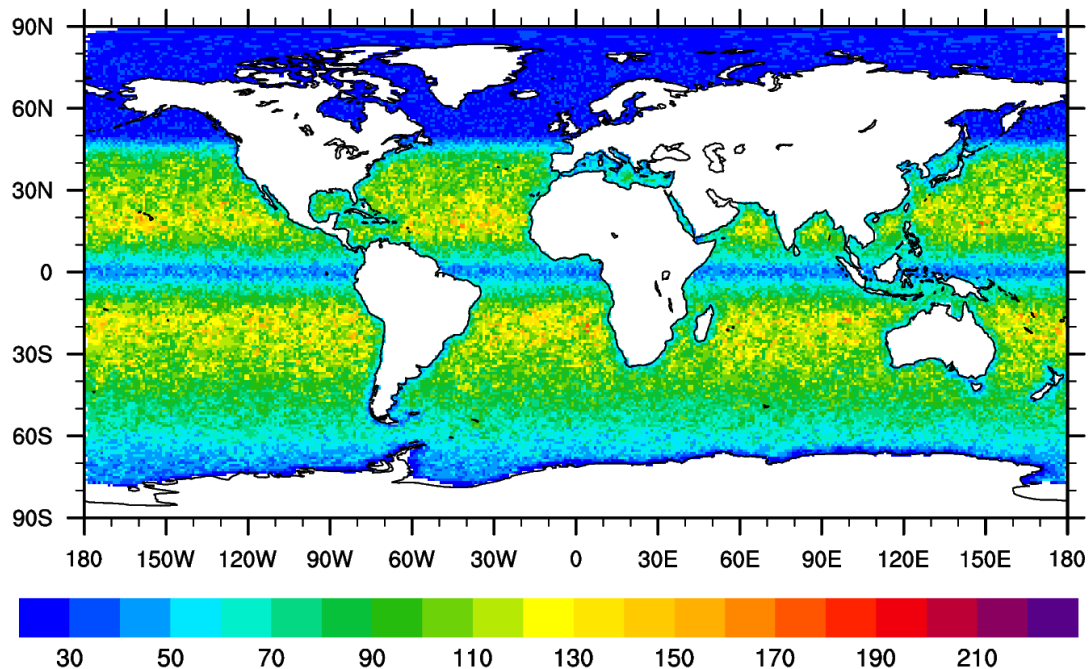
## Supplementary figures

**S1:** Excess  $^{210}\text{Pb}$  activity from the sediment cores with depth in dpm (disintegration per minute) per gram with error bars ( $1\sigma$ ).

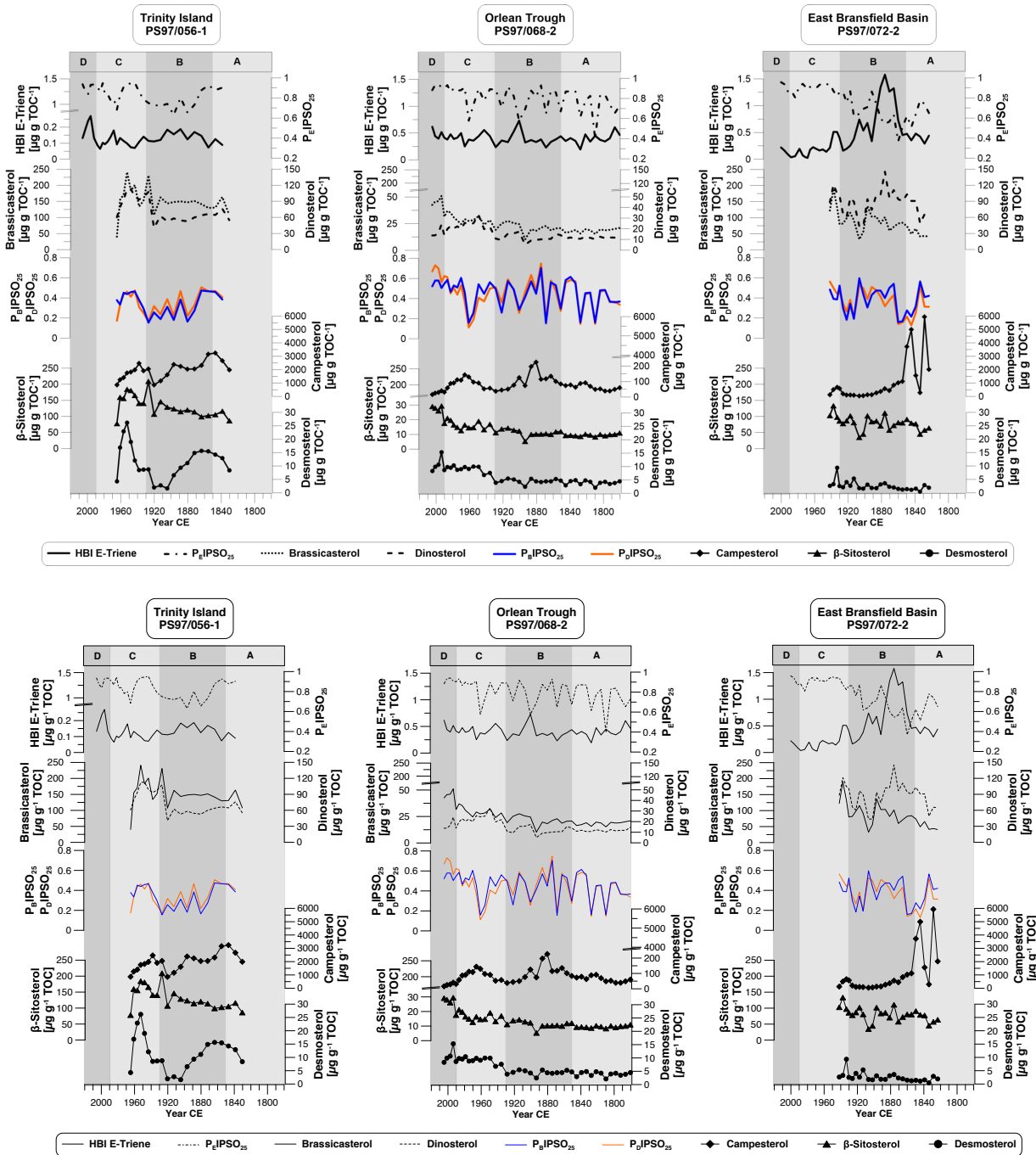


5

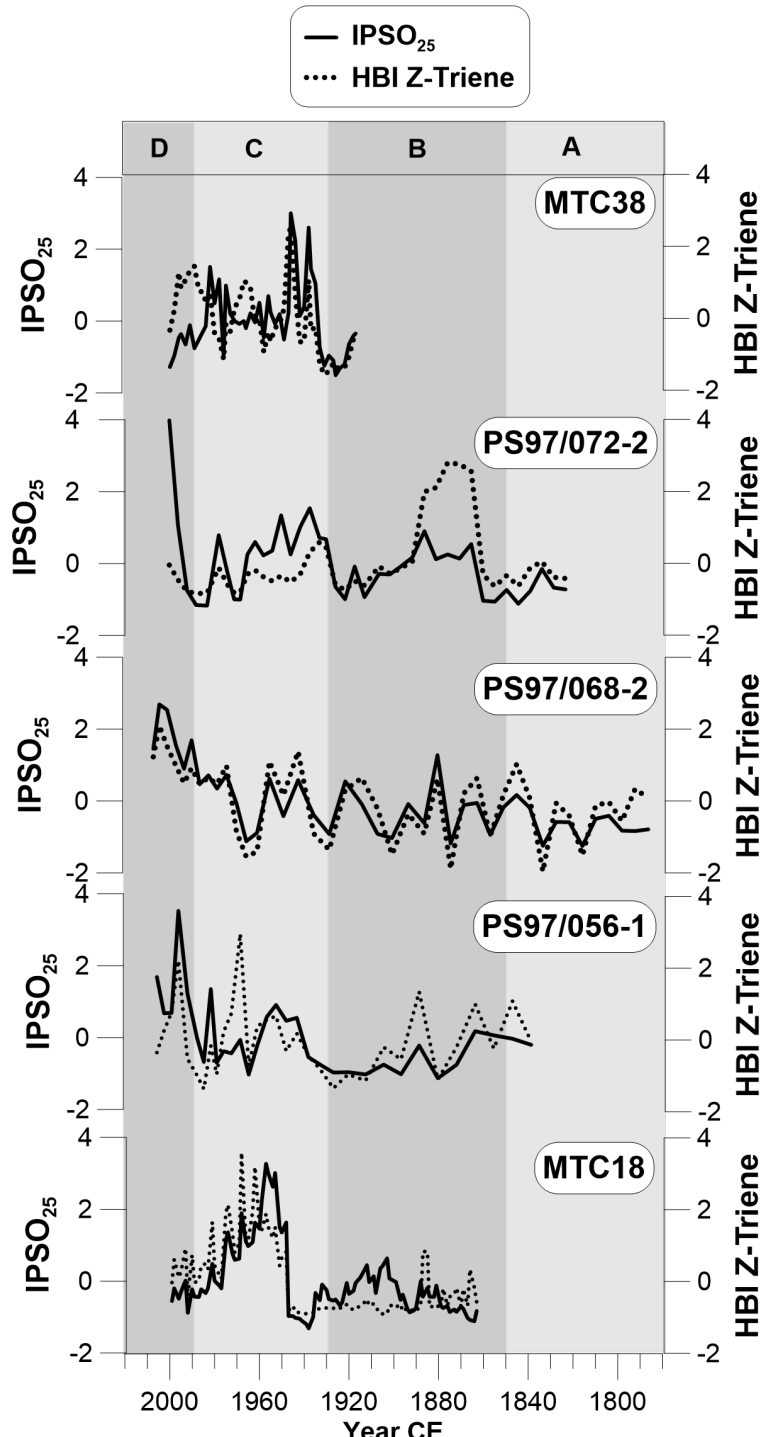
**S2:** The resolution of the ocean model in AWI-ESM2.



**S3: Additional analytical biomarker results from all three core sites including (from top to bottom) HBI E-trienes, the sea ice index  $P_E\text{IPSO}_{25}$ , brassicasterol and dinosterol (Kanazawa et al., 1971; Volkman, 2003) with their according sea ice indices  $P_B\text{IPSO}_{25}$  and  $P_D\text{IPSO}_{25}$ , respectively. The terrestrial biomarkers campesterol and  $\beta$ -sitosterol (Volkman, 1986) were not used for sea ice estimations. Desmosterol is suspected to be related to sea ice (Cárdenas et al., 2019) but was not considered in our discussion as well. Vertical grey bars denote the stratigraphic units A to D.**



S4: The normalized biomarker  $\text{IPSO}_{25}$  and HBI Z-triene from eastern AP (MTC38A) and western AP (MTC18A) (Barbara et al., 2013) compared to biomarker records from this study. High biomarker concentrations are evident in all records since 1930, or later, pointing to a shift towards an environment with dynamic sea ice seasons supporting higher primary production. Vertical grey bars denote the stratigraphic units A to D.



**S5:** Additional numerical model data from spring sea ice thickness (mSSIT, 10 year running mean) and surface air temperature (mSAT, 10 year running mean) from all three core sites. Vertical grey bars denote the stratigraphic units A to D.

